Journal Name

ARTICLE

Developing a self-healing supramolecular nucleoside hydrogel

K. J. Skilling, [a] B. Kellam, [a] M. Ashford, [b] T. D. Bradshaw [a] and M. Marlow [a]

Received 00th January 20xx,
Accepted 00th January 20xx

DOI: 10.1039/x0xx00000x

www.rsc.org/

Low molecular weight gelator hydrogels provide a viable alternative to traditional polymer based drug delivery platforms, owing to their tunable stability and in most cases inherent biocompatibility. Here we report the first self-healing nucleoside hydrogel using *N4*-octanoyl-2'-deoxycytidine (0.5 % *w/v*) for drug delivery. The hydrogel's cross-linked nanofibrillar structure, was characterised using oscillatory rheology and confirmed using SEM and TEM imaging . The potential of this gel for drug delivery was explored *in vitro* using fluorescently labelled tracers. Cell viability assays were conducted using pancreatic cell lines which tolerated the gels well; whilst no adverse effects on the viability or proliferation of cells were observed for fibroblast cell lines.

Introduction

The versatility of low molecular weight gelators (LMWGs) makes them attractive materials for use in drug delivery. [1-3] There already exist examples of low molecular weight gelating entities with potential for use in drug delivery, whether they be therapeutic molecular gels, such as the recent linifinib[4] and benzothiazole[5] examples or inert gelator matrices such as the extensively studied tri-/dipeptide gelators. [6-8] Whilst there is extensive literature describing the applications of LMWGs in drug delivery, there are only a few published examples of these inert matrix gelators that possess self-healing properties *i.e.* the ability to reform after application of high shear. [9-11] This ability for recovery after high shear is particularly relevant for injectable gels sheared through a needle as following injection the gel would be required to revert back to its original state. Indeed the self-healing properties of LMWGs is uncommon[12] when compared to the reported self-healing of polymer hydrogels. [13-17] In the studies reported here we will describe the rare self-healing properties of a nucleoside based gelator.

Previously described gelation of acylated nucleoside gelators based on cytidine were carried out in a binary system of ethanol and water, where the ethanol content contributed 40 % to the overall solvent volume. [18] These acyl cytidine based gels displayed appropriate mechanical stability for retention at an injection site; and showed favourable nanofibre architectures for entrapment of higher molecular mass molecules and were shown to control the release of high and low molecular weight fluorescently labelled tracers. Whilst these acyl cytidine derivatives are suitable for drug delivery in cancer *i.e.* intra-tumoural drug delivery and topical drug delivery, [19] the requirement for ethanol in establishing a mechanically stable gel, made them unsuitable for broader drug delivery applications such as sub-cutaneous or ocular delivery. Indeed, there was an opportunity to create a hydrogelator, without the requirement of ethanol for gelation, based on cytidine and extending the applications of this drug delivery platform. Herein, we discuss our studies on gelation of acylated 2', 3'-dideoxycytidine (R=H, R_1=H) (B) and 2'-deoxycytidine (R=H, R_1=OH)(C) derivatives (Fig. 1) and the discovery of a self-healing hydrogelator, based upon 2'-deoxycytidne with potential applications in drug delivery and tissue engineering.

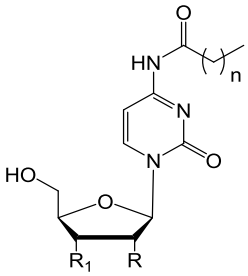

Fig. 1: Core structure of acyl derivatives of cytidine (R=OH, R_1=OH) (**A**), 2', 3'-dideoxycytidine (R=H, R_1=H) (**B**) and 2'-deoxycytidine (R=H, R_1=OH) (**C**) n = 6 to 12.

Results and discussion

The previously reported synthesis of cytidine derivatives (A), acylated at the *N4* position on the nucleobase and their subsequent gelation, in a binary system of ethanol and water, revealed that *N4*-tetradecanoylcytidine gave the most stable and reproducible gels. In this instance FTIR spectroscopy studies alluded to the amide functionality being a key functional group for gelation of *N4*-tetradecanoylcytidine, due

[a] *School of Pharmacy, University of Nottingham, NG7 2RD*
[b] *AstraZeneca, Macclesfield, Cheshire, SK10 2NA*

† Footnotes relating to the title and/or authors should appear here.
Electronic Supplementary Information (ESI) available: [details of any supplementary information available should be included here]. See DOI: 10.1039/x0xx00000x

Table 1: Structure and associated clogP and $logS_w$ values of acylated cytidine, 2', 3'-dideoxycytidine and 2'-deoxycytidine derivatives, where clogP is the calculated partition coefficient and logSw is the predicted water solubility Representative structures of all compounds are shown in Fig. 1

N4-acylated Derivatives	R	R_1	n	clogP	Predicted $LogS_w$
Cyt-*N4*-C_{14}(**D**)	OH	OH	12	4.31	-5.09
2'-dC-*N4*-C_{14}(**E**)	H	OH	12	4.61	-5.19
2'-dC-*N4*-C_{12}(**F**)	H	OH	10	3.55	-4.61
2'-dC-*N4*-C_{10}(**G**)	H	OH	8	2.49	-4.02
2'-dC-*N4*-C_8(**H**)	H	OH	6	1.44	-3.41
2'-dC-*N4*-C_6(**I**)	H	OH	4	0.38	-2.79
2',3'-ddC-*N4*-C_{14}(**J**)	H	H	12	5.26	-5.27
2',3'-ddC-*N4*-C_{12}(**K**)	H	H	10	4.20	-4.68
2',3'-ddC-*N4*-C_{10}(**L**)	H	H	8	3.14	-4.08
2',3'-ddC-*N4*-C_8(**M**)	H	H	6	2.09	-3.46

to its hydrogen bonding capabilities. [18] Typically however, hydrophobic forces are normally the predominant driving force in LMWG self-assembly in hydrogels[20] and not hydrogen bonding as the presence of protic solvents such as the aforementioned water and ethanol can disrupt the self-assembly process as the solvents compete for H-bonding interactions between the gelator molecules. However, here hydrogen bonding seems to be the dominant interaction, where the presence of a bulky hydrophobic chain appears to acts as a shielding motif from the protic solvents allowing self-assembly via H-bonding between amide functionalities. This phenomenon has been described previously for both LMWG[21] and polymer hydrogels. [22]

The hydrogen bonding capabilities of these systems were further validated using synthetic procedures as described in the supplementary data (Supplementary S1) whereby we synthesised *N4*-(3-hydroxytetradecanoyl)cytidine. This compound showed increased solubility following addition of the hydrophilic 3-hydroxyl moiety, the solubility of which was enhanced at the increased solvent volume fractions (Φ_{SOL}), particularly Φ_{EtOH} 0.40 and 0.50 where the compound appeared completely soluble (Supplementary data S4 (Fig. S1)). At a lower Φ_{EtOH} there is visual evidence of a precipitate. The absence of gelation from *N4*-(3-hydroxytetradecanoyl)cytidine in the samples containing a lower Φ_{EtOH} can be attributed to intramolecular hydrogen bonding (Supplementary data S4 (Fig. S1)) between the amide carbonyl and the 3-hydroxyl. The presence of the hydroxyl obstructs any intermolecular hydrogen bonding and prevents self-assembly, this observation also validates the amide as a key functionality in the self-assembly process. Having conclusively shown the need for the presence of an acyl chain and the amide functionality we based our studies reported herein on the core structure shown in Fig. 1, where we have extended exploration of gelation towards *N4*-acylated 2'-deoxycytidine (R=H, R_1=OH) and 2', 3'-dideoxycytidine (R=H, R_1=H)-based gelators. Synthesis of 2'-deoxycytidine and 2', 3'-dideoxycytidine conjugates allowed further elucidation of the essential requirements for gelation as the role of the specific hydroxyl groups on the ribose sugar in gelation is difficult to determine by spectroscopy. For example, in FTIR spectra broad signals associated with the hydroxyl groups of the ribose are seen at 3200 – 3550 cm^{-1}. Using *N4*-tetradecanoylcytidine (D) as a foundation, as this was the focus of our previous studies, we also synthesised *N4*-tetradecanoyl-2'-deoxycytidine (E) and *N4*-tetradecanoyl-2',3'-dideoxycytidine (J) (Table 1). Using a simple one-pot procedure adapted from previous nucleoside literature, [23] selective acylation of the exocyclic *N4*-position of the nucleobase of cytidine, [18] 2'-deoxycytidine and 2', 3'-dideoxycytidine was achieved. Vial inversion of these *N*-acyl gelators, prepared from binary mixtures of ethanol and water at solvent volume fractions (Φ_{SOL}) (0.05 to 0.50) with a low final compound concentration of 0.5 % (*w/v*), indicated moderate gelation in each series but elucidated to the differing physical nature of the gels depending upon final Φ_{SOL}. The results from gelation are suggestive of the 2'- and 3'-hydroxyl groups playing a significant role in the self-assembly process of the cytidine derived gelators as the profile of each gelator differs depending on the number of hydroxyls present on the sugar when all other conditions remain constant (see supplementary data S5).

When neither 2'- nor 3' hydroxyl functionalities are present (J) there is a reduction in the propensity for gelation at the lower Φ_{SOL}, correlating with the higher partition coefficient (clogP), lower predicted aqueous solubility ($logS_w$) and solubility driven nature of the self-assembly process. Having demonstrated that both clogP and number of hydroxyl groups on the ribose sugar influence gelation, we then synthesised a series of *N4*-acyl 2'-deoxycytidine (F-I) and *N4*-acyl-2', 3'-dideoxycytidine (K-M) derivatives (Table 1) with decreased lipophilicity and higher predicted water solubility by decreasing the length of the acyl chain introduced at the *N4*-position of the nucleobase. The effects of such modifications on gelation in binary mixtures of ethanol and water (Φ_{SOL}) (0.05 to 0.50) were then monitored. Through vial inversion screening we observed that the 2'-deoxycytidine conjugates gave gels with increased visual stability at lower Φ_{SOL} and that the most stable gels were derived from *N4*-octanoyl-2'-deoxycytidine- (2'-dC-*N4*-C_8(H)) (see supplementary data (S6)). We then further explored whether a hydrogel could be formulated in the absence of ethanol, merely with heating and cooling for 2'-dC-*N4*-C_8(H). 2'-dC-*N4*-C_8(H) was heated to just before boiling point (~95 °C) in order to fully solubilise the compound at 0.5 % (*w/v*) and then left to cool for 10 minutes prior to inversion. Fig. 2a depicts the gel following solubilisation; within 30 seconds, as the solution began to cool, the evolution of an opaque sample was noted, beginning from the bottom of the sample vial. After 2.5 minutes (Fig. 2b) a homogenous, slightly translucent system was detected. Approximately 5 minutes later (Fig. 2c) the gel once again established transparency from the bottom of the vial and after a total of 10 minutes (Fig. 2d) the gel appeared as a

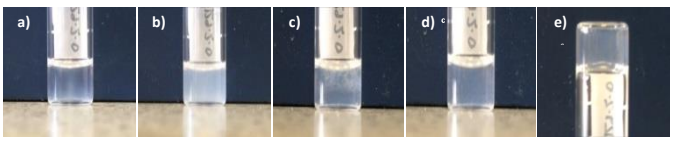

Fig. 2: Screen shot of video of gelation over 10 minutes following solubilisation of 2'-dC-*N4*-C_8(H). a) Following solubilisation b) 2.5 minutes c) 5 minutes d) 10 minutes and e) 10 minutes inverted.

homogenous transparent system, capable of retaining structural integrity upon inversion (Fig. 2e).

Similar reports of turbidity followed by a transparent gel formation have been reported in the literature; Chen *et al.* observed for fluorenylmethoxycarbonyl (Fmoc)-leucine-glycine, a turbid solution transforming to a clear gel within a few minutes. They also reported that the increase in turbidity correlated with a phase separation event forming a dispersion of spheres in solution and that the dispersion was unstable, with

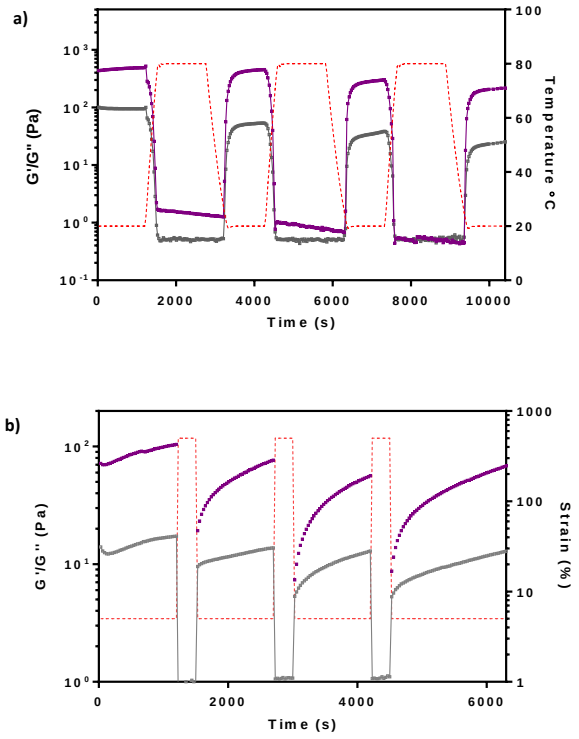

Fig. 3: Recovery sweeps of H Φ_{SOL} 0.00, 0.5 % *w/v*. a) Temperature profiling (T_{prof}) sweep. (Φ_{SOL} 0.00) was measured over 10000 seconds at a constant strain γ = 1 % and frequency ω = 10 rad/s. G' (purple) an G'' (grey) were measured between 20 and 80 °C (red) Standard Deviation (G') 234 ± 80 Pa b) Shear/ Recovery profile over 6000 seconds at a constant frequency (ω = 10 rad/s) and temperature (T = 37 °C) alternating (red) between a stable strain (5 %) and strain resulting in complete deformation of the gel (500 %). Standard Deviation (G') 188 ± 90 Pa G' (purple) and G'' (grey). In all cases n = 4

a fibrous network being formed at the expense of the spheres. [24] Orbach *et al*. also monitored, by spectroscopic analysis, the formation of the Fmoc-amino acid hydrogels through a transition from a turbid solution to a transparent network. [25] In accordance with previous data of Chen *et al*, the hypothesis emerged that restructuring of the matter occurred, from multiple irregular aggregates possessing dimensions in the range of the visible wavelength into highly ordered structures, causing the optical characteristics of the solution to change. Most recently Draper *et al.* reported a 2-thiophene diphenylalanine gel that showed this transition from a turbid to translucent gel over 3 days. [26]

Following the qualitative stability to inversion tests and the comparatively fast gel formation over 10 minutes, 2'-dC-*N*-C_8(H) was analysed using oscillatory rheology to characterise the strength of the gels, important for our intended drug delivery application. [1] Strain/amplitude and frequency sweep oscillatory tests at a physiological 37 °C were used to verify the viscoelastic behaviour of the gelator (Supplementary data; S7 Fig. S2). Notably there was an order of magnitude between G' and G'' which is a characteristic of LMWGs **[27]** and a maximal G' value of 20 Pa, making it mechanically weaker than previous acyl cytidine derivatives[18] but a comparable magnitude to the guanosine and deoxy-guanosine gelators reported by Adhikari *et al.* [9] The low G' value of this soft hydrogel is more indicative of entanglement of fibres than a crosslinked network. [28] Indeed, entanglement of fibres with transient crosslinks may be responsible for the most interesting behaviour of this *N4*-octanoyl-2'-deoxycytidine gel as demonstrated by temperature profiling and time dependent-recovery tests. Temperature profiling (Fig. 3a) was undertaken to determine whether the number of heat cool cycles would alter previously observed mechanical strength. In this instance the temperature was alternated between ambient temperature (20 °C) at which we knew the hydrogel was self-supporting and 80 °C at which we knew the gelator was known to be in solution. There was no significant reduction in mechanical strength following 3 heat-cool cycles and the gel recovered within 2-3 minutes. Fig. 3b also depicts a time-dependent recovery test; recovery occurs when the molecules are no longer under high strain and are able to return to the kinetically favoured structure identified prior to deformation. The gels were subjected to alternating strains; 5 % at which the gel is within the linear viscoelastic region (for 1200 s) and then at 500 % at which point complete breakdown of the gelator network to a liquid state (300 s) would be expected. However, we observed, after releasing a high strain and after a suitable relaxation phase, the gel demonstrated a mechanical strength recovery ratio of 0.70 following each heat-cool cycle. This capacity for recovery after high shear is particularly relevant for injectable gels sheared through a needle as following injection the gel would be required to revert back to its original state. Although this self-healing property has been extensively reported for polymeric systems, [13-17] there are fewer reports for LMW gels. [9-11] Pertinent examples are dipeptide gels (Fmoc-Leucinylglycine and Fmoc-phenylalaninylphenylalanine) which have been shown to recover after shear in similar experiments. Additional literature supports the mechanism for self-healing gels being associated

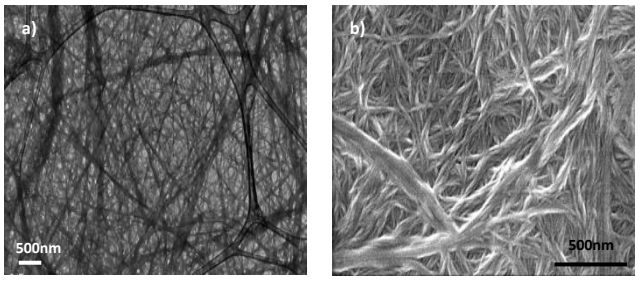

Fig. 4: Electron microscopy images of 2'-dC-*N4*-C (H) a) Transmission electron microscope (TEM) image of a highly entangled fibre network and b) scanning electron microscope (SEM) image of gelator surface. The scale bars represent 500 nm in both images

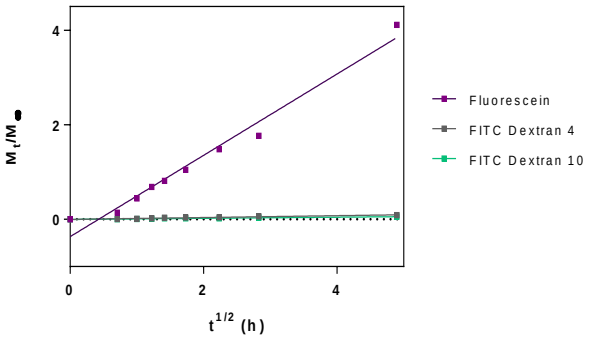

Fig. 5: Release kinetics of Fluorescein (0.08 mM), FITC Dextran 4 (0.005 mM) and FITC Dextran 10 (0.005 mM) through the gel matrix of 2'-dC-*N4*-C_8(H)

with those systems formed by a nucleation and growth process, as also shown here for the 2'-dC-*N*-C_8 (H) gelator (Fig. 2). Similarly relationships were also shown for oligopeptide gels of Yan *et al.* [29] Following on from these promising recovery-after-shear profiles, microscopy studies (SEM and TEM) were then undertaken to investigate gel properties with respect to the presence of a cross-linked fibre network containing cavities suitable for encapsulation of therapeutic materials. These microscopic cavities were accordingly confirmed by TEM and SEM within the gelator matrix of 2'-dC-*N4*-C_8(H) (Φ_{SOL} 0.00) (Fig. 4). Further analysis of these images quantified each fibre to have an approximate width of between 20 and 25 nm,

Table 2: Solution phase growth inhibition studies for 2'-deoxycytidine and 2'-dC-*N4*-C_8 in MIA PaCa-2, MKN-7 and MCF-7 adenocarcinoma cell lines, where GI_{50} represents the concentration at which the test agent inhibits cell growth by 50 %. Assays were carried out in n = 3.

	GI_{50} (mM)		
Compound	MIA PaCa-2	MKN-7	MCF-7
2'-deoxycytidine	9.55 ± 3.65	9.99 ± 2.81	4.14 ± 2.47
2'-dC-*N4*-C_8	6.58 ± 1.40	7.74 ± 3.26	3.94 ± 0.74

and a length of approximately 200 µm Having confirmed the presence of nanofibres and macroscopic cavities, *in vitro* release was evaluated using fluorescein (332 Da), fluorescein isothiocyanate dextran 4000 Da (FITC dextran 4) and fluorescein isothiocyanate dextran 10000 Da (FITC Dextran 10). The fluorescent molecules were solubilised in the aqueous phase to a final gel volume of 2 mL during gel preparation and formulated at 0.5 % (*w/v*) using the aforementioned heating and cooling procedure. Upon cooling to ambient temperature, phosphate buffered saline (PBS, 5 mL) was placed on top of the gel and the release monitored over 24 h by removing aliquots (150 µL) of the free aqueous phase at specific intervals and measuring the relative fluorescence. The sample volume was small relative to the final volume of the free aqueous phase so as not to disturb the environment. The release of the fluorescent tracers was monitored over time by calculating the diffusion coefficients using the non-steady state diffusion equation reported elsewhere, [8,12] where M_t is the total number of molecules released from the matrix between time points, $M\infty$ is the total number of molecules left in the matrix.

Release from a hydrogel can be controlled by many factors, including the size of the cavities in the mesh network, the surface area to volume ratios, molecular weight of trapped compounds and interactions between the gel matrix and entrapped molecules. Over the time course of the release no change was observed in the macro structure of the gel *i.e.* no swelling, shrinking or gel degradation. Fig. 5 shows the amount of fluorescent tracer released plotted against the square root of time. There is a good linear relationship between the amounts of fluorescein dye released over time showing $R^2 > 0.97$ indicating that again the release profile follows Fickian diffusion. The total percentage release of each fluorescein from the gel matrix was 67 % after 24 h, whereas the release of the two FITC Dextran compounds was < 5 %. The retarded release of the FITC Dextran compounds can be attributed to their high molecular weight and the closely-packed structure of the fibres within the gel matrix trapping them in place. The diffusion coefficient was calculated from the linear regression analysis of the fluorescein release profile. The calculated diffusion coefficient of fluorescein ($0.19 \pm 0.004 \times 10^{-10}$ m^2/s) is similar to that previously reported in literature for other drugs and drug-like molecules, where values were seen to be in the range of 2.9×10^{-11} and 5.6×10^{-10} m^2/s. [23] This value also correlates to those previously reported in literature for the release of fluorescein from Fmoc-dipeptide hydrogels. [8,30] The diffusion coefficients of FITC dextran 4 and FITC dextran 10 were not calculated as only minimal release was detected over the 24 h sampling period.

To confirm the biocompatibility of 2'-dC-*N4*-C_8(H) and hence its suitability for drug delivery, *in vitro* studies were then carried out using mammalian cell growth inhibition assays (Table 2). Firstly, solutions of the gelator where used to determine the concentration of test agent at which cell growth or net proliferation is inhibited by 50 % (GI_{50}) for MCF-7 human breast adenocarcinoma, MIA PaCa-2 human pancreatic carcinoma and MKN-7 human stomach adenocarcinoma (Table 3). Negligible detrimental effects of gelator solutions on cell growth and viability were observed: indeed, millimolar GI_{50} concentration values were found for both 2'-deoxycytidine and 2'-dC-*N4*-C_8 in each of the tested cell lines, with 2'-dC-*N4*-C_8 causing slightly more growth inhibition than the parent compound in every tested cell line.

Having confirmed the concentration of the gelator in solution for growth inhibition, the impact of 0.5 % and 1 % (*w/v*) gels; as a deposit onto a cell monolayer and as a 'raft' in medium, on MIA PaCa-2 and MRC-5 human fibroblast cell lines was examined (Fig. 6). The volume of gel injected was calculated to give two final concentrations which matched the GI_{50} and 2 × GI_{50} concentrations as determined for 2'-dC-*N4*-C_8 in solution. The results after 24 h in MIA PaCa-2 cells show a notable difference in the observed absorbance between those cells in contact with the gel and those exposed to the gel 'raft'. Both 0.5 % and 1 % (w/v) gels injected on to the cell monolayer displayed an approximate 50% reduction in cell growth whilst less growth inhibition was found for those cells those exposed to the gel 'raft'. Also observed in Fig. 6, is increased proliferation of cells up to 48 h under all gel conditions, signifying that the viable cells tolerate exposure to the gels well ≤ 48h.

MRC-5 results are also depicted in Fig. 6. Fibroblasts were seen to grow to a maximum density after 24 h as demonstrated by comparison with a live control. This density was maintained for a further 48 h and the presence of the gel was found to have no adverse effect on the viability or proliferation of cells under any of the tested conditions.

Conclusions

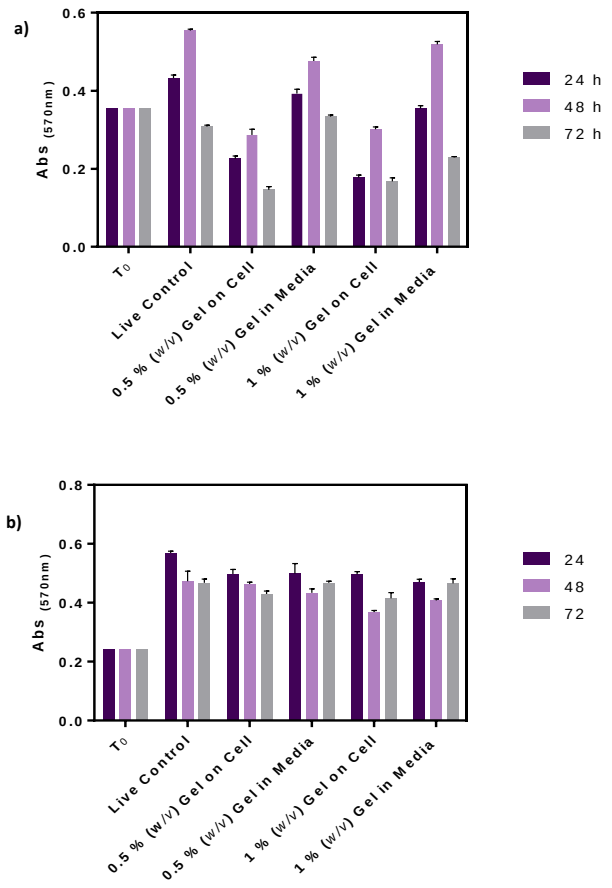

Fig. 6: Cell proliferation colorimetric assay of gels made from 2'-dC-*N4*-C8 (0.5 % and 1 % *w/v*) injected on to the cell monolayer and in suspended in RPMI-1640. a) MIA PaCa-2 human pancreatic adenocarcinoma cells and b) MRC-5 human fibroblast cells. Assays were carried out in n = 3. Paired t-test analyses were run on the 72 h time points **** p < 0.0001

Previously reported was the gelation of acyl cytidine derivatives in a binary system of ethanol and water. Having shown the need for the presence of an acyl chain and the amide functionality, our studies herein were based on acylated 2', 3'-dideoxycytidine and 2'-deoxycytidine based gelators with lower clogP values and increased predicted water solubility to further explore our goal of finding a functional nucleoside hydrogelator. Accordingly, we reported *N4*-octanoyl 2'-deoxycytidine, which formed a stable gel in water following a heating and cooling procedure. Rheological testing confirmed this system to be stable under relatively high strains and demonstrated the propensity of the gel to act as a 'self-healing' material, thus validating it for use as a potential drug delivery system. Further electron microscopy imaging confirmed the nanostructure to be a cross-linked fibrous network and *in vitro* release studies demonstrated a diffusion-mediated release of small molecular weight fluorescein from the gelator matrix, whilst larger molecular weight FITC dextran 4 and 10 were retained. *In vitro* growth inhibition assays finally established the gel scaffold as an inert matrix and thus confirmed the suitability of the hydrogel for drug delivery applications.

Experimental section

Materials

2'-deoxycytidine was purchased from TCI Chemicals (Europe) and all other chemicals and solvents were purchased from commercial suppliers and used without further purification. 1.5 mL sample vials were purchase from Fischer Scientific, 7 mL aluminium rheology vials were purchased from Anton Paar GmBh and Transmission electron micrograph grids were purchased from EM Resolutions

Methods

General Methods. ^{1}H NMR spectra were recorded on a Bruker 400 Ultrashield at 400.13 MHz at 25 °C. ^{13}C NMR spectra were recorded on a Bruker AV(III) at 500 MHz at 25 °C. Unless stated otherwise, solvent used for NMR analysis was DMSO-*d6* ($(CHD_2)2SO$ at δH 2.50 ppm, $(CD_3)2SO$ at 39.52 ppm). Chemical shifts (δ) are recorded in parts per million (ppm). Coupling constants (*J*) are recorded in Hz (rounded to one decimal place) and any significant multiplicities described by singlet (s), doublet (d), triplet (t), quadruplet (q), broad (br), multiplet (m), doublet of doublets (dd) and doublet of triplets (dt). Spectra were assigned using correlation spectroscopy (COSY) sequences. Melting points (m.p.) were recorded on a Gallenkamp Melting point apparatus and were corrected using benzoic acid as a standard (121 – 123 °C). High Resolution Mass Spectroscopy (HRMS) time of flight, electrospray (TOF ES +/-) was recorded on a Waters 2795 separation module micro-mass LCT platform. Analytical Reverse Phase High Performance Liquid Chromatography (RP-HPLC) mobile phases were prepared as follows: Eluent A – 0.05 % trifluoroacetic acid (TFA) (*v/v*) in water sonicated for 30 min; Eluent B – Eluent A in CH_3CN (1:9) sonicated for 30 min. All RP-HPLC gradients were performed using a Waters 2767 sample manager, Waters 2525 binary gradient module and visualised at 254 nm with a Waters 2487 dual wavelength absorbance detector and spectra were analysed using MassLynx. A YMC-Pack C8 column (150 mm × 4.6 mm × 5 µm) at a flow rate of 1 mL/min was used to collect the data. The retention time (t_R) of the final product is reported in minutes using a gradient of 0 – 1 min 5 % solvent B in solvent A, 2 – 26 min gradient of 5% to 90 % solvent B in solvent A, 27 – 35 min held at 90 % solvent B in solvent A, 35 - 36 min 90 % to 5 % solvent B in solvent A, 36 - 38 min held at 5 % solvent B in solvent A (solvent A = 0.05 % TFA in H_2O, solvent B = 0.05 % TFA in 9:1 *v:v* CH_3CN:H_2O). Purities of all compounds tested were determined by RP-HPLC to be ≥ 95 %.

Synthesis of *N4*-octanoyl-2'-deoxycytidine (2'-dC-*N4*-C_8). To a solution of 2-chloro-4,6-dimethoxy-1,3,5-triazine (CDMT, 1.1 mmol, 1 eqv, 193 mg) in anhydrous CH_2Cl_2 (3.5 mL) at 0 °C, was added *N*-methylmorpholine (NMM, 1.50 mmol, 1.36 eqv, 171 µL) with continuous stirring until a white suspension had formed. The mixture was then left to stir for 1 h. Octanoic acid (1.1 mmol, 1 eqv, 159 mg, 179 µL) was added directly into the mixture as a solution in anhydrous DMF (2 mL) and stirred for a further hour. A solution of 2'-dC-*N*-C_8 (H) (1.1 mmol, 1 eqv, 250 mg) in anhydrous DMF (2 mL) was made up at 0 °C. The cold triazine solution was added drop wise to the cooled cytidine solution over 30 mins, before heating to 50 °C and stirring for 7-8 h. The cooled solution was evaporated *in vacuo*. The product was purified using flash silica column chromatography, eluting at 5 - 8% methanol in CH_2Cl_2

^{1}H NMR (DMSO-d_6) δ 0.86 (t, J = 6.8 Hz, 3H, CH_3), 1.25 (br-m, 8H, CH_2-$(CH_2)_4$-CH_3), 1.46-1.60 (m, 2H, C=O-CH_2-CH_2), 1.98-2.31 (m, 2H, HO-CH-CH_2), 2.38 (t, J = 7.4 Hz, 2H, C=O-CH_2), 3.53 - 3.64 (m, 2H, 5'-CH_2), 3.85 (q, J = 3.8 Hz, 1H, 4'-CH), 4.21 (m, 1H, 3'-CH), 5.03 (t, J = 5.3 Hz, 1H, 5'-OH), 5.25 (d, J = 4.2 Hz, 1H, 3'-OH), 6.10 (t, J = 6.3 Hz, 1H, 1'-CH), 7.22 (d, J = 7.4 Hz, 1H, 6-CH), 8.31 (d, J = 7.5 Hz, 1H, 5-CH), 10.81 (s, 1H, NH). ^{13}C NMR (DMSO-d_6) δ 14.40, 22.51, 24.93, 28.85, 28.89, 31.58, 36.81, 61.41, 70.40, 86.59, 88.36, 95.72, 145.42, 150.38, 154.93, 162.74, 174.39. *m/z*: HRMS (TOF ES+) $C_{17}H_{28}N_3O_5$ $[M+H]^+$ calculated 354.2023; found 353.7968. m.p: 122 – 125 °C. Analytical RP-HPLC t_R = 16.4 min, Yield: 42.0 %, 97.3 % purity.

Hydrogel preparation. Stability to inversion was carried out by weighing samples using an A and D GR-202 semi micro-analytical balance into 1.5 mL sample vials. *N4*-octanoyl-2'-deoxycytidine (2'-dC-N4-C_8(H) (2.5 mg) was dispersed in ultra-purified water (500 µL), sample was sonicated for 1 – 2 min before being heated to approximately 95 °C or until compound had completely solubilised. Sample was then left to cool to room temperature prior to inversion.

Rheological measurements Rheology was carried out using an Anton Paar MCR302 Modular Compact Rheometer. A four-bladed vane geometry was used with a diameter of 8.5 mm and length 8.5 mm in a cup with a diameter of 14.5 mm. The solution of gelator was prepared in 7 mL aluminium cups to a final sample volume of 2 mL, as per the method described above. Once the gel was prepared, the sample vial was mounted in the lower plate (cup) of the rheometer; the vane (attached to the upper part) was lowered into place, at a depth of 2 mm. This arrangement gave a total sample depth of approximately 16 mm in the 14.5 mm diameter cup which allowed positioning of the vane in the centre of the sample. All rheological measurements were carried out in 7 mL aluminium vials to allow for heating of the sample prior to measurement.

Strain sweeps were carried out between γ = 0.05 - 100 % at a constant angular frequency of 10 rad/s. Frequency sweeps were executed from 0.1 to 100 rad/s at a constant strain of 5 %, as dictated by the linear viscoelastic region from the strain sweep. Both strain and frequency measurements were carried out at 37 °C to mimic physiological conditions. Temperature profile ($T_{profile}$) measurements were carried out by alternating the system temperature between 20 and 80 °C at 20 minute intervals at constant strain (5 %) and constant frequency (10 rad/s). Time dependant recovery measurements were carried out by alternating the strain between 5 % and 500 %; conditions that could guarantee a stable gel at the lower strain and complete deformation at the higher strain. The strains were applied in 20 min (5 %) and 5 min (500 %) cycles. The frequency (10 rad/s) and temperature (37 °C) were kept constant throughout.

Electron Microscopy. Scanning electron microscopy (SEM) was performed on a JEOL JSM-6060LV compact scanning electron microscope. All samples were loaded onto suitable stub holders with a 200 µL micropipette fitted with sterile tips. The point of the tip was cut to increase the diameter and thus minimize the shear stress applied to the gels. The stubs were sputter coated with gold (Balzers Benchtop sputter coater SCD 030) under an argon atmosphere (50 Pa) at 30 mA for 4 mins before imaging. Images were acquired using an electron beam of 7–22 kV. Transmission electron microscopy (TEM) was carried out by dispersing a small amount of gel in 150 µL of ultra-purified water and pipetting on to a graphene oxide, lacey carbon coated copper grid (No. 300). Excess sample was blotted with Whatman 50 filter paper. The grid was subjected to high vacuum in a Gatan dry pumping station (model 655) prior to inserting into the machine and imaging at an accelerated voltage of 100 kV.

In vitro release kinetics of fluorescent agents. Gels containing fluorescent dyes were prepared in 7 mL Aluminium cups to a final gel volume of 2 mL with the dye phase replacing the aqueous phase in each instance. Stock solutions of each dye were prepared so that the fluorescent output would be within the linear region of the calibration curves (0.15 mM Fluorescein and 0.06 mM Fluorescein isothiocyanate (FITC) dextran 4 kDa and 0.08 mM FITC dextran 10 kDa. The gel volume was allowed to stand for 18 h to allow time for complete gelation. PBS (5 mL) was gently placed on top of each gel and the initial time point taken (150 µL, T_0), subsequent readings (150 µL) were taken at further time points. After each time point the buffer volume (150 µL) was replaced and the fluorescence measured (excitation of 485 nm with the emission measured at 521 nm) using a Perkin Elmer plate reader.

In vitro growth inhibition assays. MCF-7 human breast adenocarcinoma, MIA PaCa-2 human pancreatic carcinoma and MKN-7 human stomach adenocarcinoma cell lines were cultured in RPMI-1640 medium supplemented with 10 % Foetal Bovine Serum (FBS). MRC-5 human fibroblast cells were cultured in modified eagles medium (MEM, containing sodium bicarbonate) supplemented with 10 % heat inactivated foetal calf serum, 1% penicillin/streptomycin, 1 % L-glutamine (200 mM), 1 % non-essential amino acids (0.1 nM), 1 % 4-(2-hydroxyethyl)-1-piperizineethanesulfonic acid (HEPES) buffer (1 M) and 1 % sodium bicarbonate (7.5 %). Cells were passaged upon reaching 60 - 80% confluency and not used passed passage number 50. MTT was made in sterile PBS at a concentration of 2 mg/mL.

Solution State assays: Cells were seeded at a density of 3×10^3 cells per well into 96-well microtiter plates and allowed to adhere for 24 h before test agent was introduced (0.5 mM – 20 M, n = 8). Stock solutions of each compound were prepared in DMSO to aid solubilisation and further dilutions were prepared in RPMI-1640 medium prior to each assay. At the time of agent addition a control sample was treated with 3-(4,5-dimethylthiazol-2-yl)-2,5-diphenyltetrazolium bromide (MTT) (final concentration 400 μg/mL) to generate T_0 sample readings. Cells were incubated with test agent for 72 h at 37 °C and 5 % CO_2. Following this exposure MTT was added to each well (final concentration 400 μg/mL) and re-incubated at 37 °C for 2.5 h to allow reduction of MTT by viable cells (mitochondrial dehydrogenases) to insoluble formazan crystals. Well supernatants were removed, and intracellular formazan solubilized by addition of DMSO (150 μL). Absorbance was read at 550 nm using a Perkin Elmer plate reader. Non-linear regression analysis was used to calculate compound concentrations required to inhibit 50 % of cell growth (GI_{50}).

Gels injected onto cells: Gels of *N4*-octanoyl-2′-deoxycytidine-(2′-dC-N4-C_8(H)were made as previously described of 0.5 % and 1 % (*w/v*) in RPMI-1640 medium. However, before leaving to cool the solution was transferred into a 1 mL syringe through a 19G needle and left for 18 h at ambient temperature.

MIA PaCa-2 carcinoma cells and MRC-5 fibroblasts were seeded at a density of 1×10^5 and 5×10^5 cells/well, respectively. Plates were incubated (37 °C and 5 % CO_2) for 24 h prior to introduction of the gel. MRC-5 cells were chosen as a control cell line, representative of healthy tissue. Both concentrations (0.5 % and 1 % *w/v*) were tested as i) a deposit on to the cell monolayer where the medium was aspirated and each gel injected on to the cells and then media reintroduced ii) a raft where the gel was injected directly into the cell culture medium. 50 μL of gel was used to give two final concentrations which matched the GI_{50} and $2 \times GI_{50}$ concentrations *N4*-octanoyl-2′-deoxycytidine (2′-dC-N4-C_8(H)) as determined by MTT. The plates were then incubated at 37 °C and 5 % CO_2. At the time of gel addition a control sample was treated with MTT (final concentration 400 μg/mL) to generate a T0 sample reading. At 24, 48 and 72 h time points MTT (final concentration 400 μg/mL) was added to each cell containing well and the plates again incubated for a further 2.5 h to allow reduction of MTT by viable cells (mitochondrial dehydrogenases) to insoluble formazan crystals. Well supernatants were removed, and intracellular formazan solubilised by addition of DMSO (300 μL). Absorbance was read at 550 nm using a Perkin Elmer plate reader.

Acknowledgements

Support from Mike Fay at the Nottingham Nanotechnology and Nanoscience Centre (NNNC) for the TEM Imaging is gratefully acknowledged. Funding was provided by EPSRC (EP/I01375X/1) and AstraZeneca.

Notes and references

1. K. J. Skilling, F. Citossi, T. D. Bradshaw, M. Ashford, B. Kellam and M. Marlow, *Soft Matter*, 2014, **10**, 237-256.
2. R. Tian, J. Chen and R. Niu, *Nanoscale*, 2014, 6, 3474-3482.
3. B. Xu, *Langmuir*, 2009, **25**, 8375-8377.
4. M. Marlow, M. Al-Ameedee, T. Smith, S. Wheeler and M. J. Stocks, *Chemical Communications*, 2015, **51**, 6384-6387.
5. E. L. Stone, F. Citossi, R. Singh, B. Kaur, M. Gaskell, P. B. Farmer, A. Monks, C. Hose, M. F. G. Stevens, C.-O. Leong, M. Stocks, B. Kellam, M. Marlow and T. D. Bradshaw, *Bioorganic & Medicinal Chemistry*, 2015, **23**, 6891-6899.
6. D. J. Adams, *Macromolecular Bioscience*, 2011, **11**, 160-173.
7. G. L. Liang, Z. M. Yang, R. J. Zhang, L. H. Li, Y. J. Fan, Y. Kuang, Y. Gao, T. Wang, W. W. Lu and B. Xu, *Langmuir*, 2009, **25**, 8419-8422.
8. S. Sutton, N. L. Campbell, A. I. Cooper, M. Kirkland, W. J. Frith and D. J. Adams, *Langmuir*, 2009, **25**, 10285-10291.
9. B. Adhikari, A. Shah and H.-B. Kraatz, *Journal of Materials Chemistry B*, 2014, 2, 4802-4810.
10. A. J. Kleinsmann, N. M. Weckenmann and B. J. Nachtsheim, *Chem.-Eur. J.*, 2014, **20**, 9753-9761.
11. J. Raeburn, C. Mendoza-Cuenca, B. N. Cattoz, M. A. Little, A. E. Terry, A. Zamith Cardoso, P. C. Griffiths and D. J. Adams, *Soft Matter*, 2015, 11, 927-935.
12. Y. Nagai, L. D. Unsworth, S. Koutsopoulos and S. Zhang, *Journal of Controlled Release*, 2006, **115**, 18-25.
13. E. A. Appel, J. del Barrio, X. J. Loh and O. A. Scherman, *Chemical Society Reviews*, 2012, **41**, 6195-6214.
14. M. Guvendiren, H. D. Lu and J. A. Burdick, *Soft Matter*, 2012, **8**, 260-272.
15. H. L. Lim, Y. Hwang, M. Kar and S. Varghese, *Biomaterials Science*, 2014, **2**, 603-618.
16. S. Merino, C. Martin, K. Kostarelos, M. Prato and E. Vazquez, *Acs Nano*, 2015, **9**, 4686-4697.
17. Y. Yang and M. W. Urban, *Chemical Society Reviews*, 2013, **42**, 7446-7467.
18. K. J. Skilling, A. Ndungu, B. Kellam, M. Ashford, T. D. Bradshaw and M. Marlow, *Journal of Materials Chemistry B*, 2014, **2**, 8412-8417.
19. M. Rodrigues, A. C. Calpena, D. B. Amabilino, M. L. Garduno-Ramirez and L. Perez-Garcica, *Journal of Materials Chemistry B*, 2014, **2**, 5419-5429.
20. L. A. Estroff and A. D. Hamilton, *Chemical Reviews*, 2004, **104**, 1201-1217.
21. H. Fenniri, P. Mathivanan, K. L. Vidale, D. M. Sherman, K. Hallenga, K. V. Wood and J. G. Stowell, *J Am Chem Soc*, 2001, **123**, 3854-3855.
22. T. V. Chirila, H. H. Lee, M. Oddon, M. M. L. Nieuwenhuizen, I. Blakey and T. M. Nicholson, *Journal of Applied Polymer Science*, 2014, **131**, 39932 (1-12)..
23. J. J. Panda, A. Mishra, A. Basu and V. S. Chauhan, *Biomacromolecules*, 2008, **9**, 2244-2250.
24. L. Chen, J. Raeburn, S. Sutton, D. G. Spiller, J. Williams, J. S. Sharp, P. C. Griffiths, R. K. Heenan, S. M. King, A. Paul, S. Furzeland, D. Atkins and D. J. Adams, *Soft Matter*, 2011, **7**, 9721-9727.

25. R. Orbach, I. Mironi-Harpaz, L. Adler-Abramovich, E. Mossou, E. P. Mitchell, V. T. Forsyth, E. Gazit and D. Seliktar, *Langmuir*, 2012, **28**, 2015-2022.
26. E. R. Draper, T. O. McDonald and D. J. Adams, *Chemical Communications*, 2015, **51**, 6595-6597.
27. G. Yu, X. Yan, C. Han and F. Huang, *Chemical Society Reviews*, 2013, **42**, 6697-6722.
28. N. Tzokova, C. M. Fernyhouph, P. D. Topham, N. Sandon, D. J. Adams, M. F. Butler, S. P. Armes and A. J. Ryan, *Langmuir*, 2009, **25**, 2479-2485.
29. C. Q. Yan, A. Altunbas, T. Yucel, R. P. Nagarkar, J. P. Schneider and D. J. Pochan, *Soft Matter*, 2010, **6**, 5143-5156.
30. A. Mahler, M. Reches, M. Rechter, S. Cohen and E. Gazit, *Advanced Materials*, 2006, **18**, 1365-1370.